

Postnatal regulation of germ cells by activin: The establishment of the initial follicle pool

Sarah K. Bristol-Gould^{a,1}, Pamela K. Kreeger^{b,1}, Christina G. Selkirk^c, Signe M. Kilen^c,
Robert W. Cook^a, Jingjing L. Kipp^d, Lonnie D. Shea^{b,e,f},
Kelly E. Mayo^{c,d,e,f}, Teresa K. Woodruff^{a,c,d,e,f,g,*}

^a Department of Neurobiology and Physiology, Northwestern University, Evanston, IL 60208, USA

^b Department of Chemical and Biological Engineering, Northwestern University, Evanston, IL 60208, USA

^c Center for Reproductive Science, Northwestern University, Evanston, IL 60208, USA

^d Department of Biochemistry, Molecular Biology and Cell Biology, Northwestern University, Evanston, IL 60208, USA

^e Robert H. Lurie Comprehensive Cancer Center of Northwestern University, Chicago, IL 60611, USA

^f Center for Reproductive Research, Northwestern University, Evanston, IL 60208, USA

^g Department of Medicine, Feinberg School of Medicine, Northwestern University, Chicago, IL 60611, USA

Received for publication 7 March 2006; revised 13 June 2006; accepted 14 June 2006

Available online 17 June 2006

Abstract

Mammalian females enter puberty with follicular reserves that exceed the number needed for ovulation during a single lifetime. Follicular depletion occurs throughout reproductive life and ends in menopause, or reproductive senescence, when the follicle pool is exhausted. The mechanisms regulating the production of a species-specific initial follicle pool are not well understood. However, the establishment of a follicular reserve is critical to defining the length of reproductive cyclicity. Here we show that activin A (rh-ActA), a known regulator of follicle formation and growth *in vitro*, increased the number of postnatal mouse primordial follicles by 30% when administered to neonatal animals during the time of germline cyst breakdown and follicle assembly. This expansion in the initial follicle pool was characterized by a significant increase in both germ cell and granulosa cell proliferation. However, the excess follicles formed shortly after birth did not persist into puberty and both adult rh-ActA- and vehicle-treated animals demonstrated normal fertility. A follicle atresia kinetic constant (k_A) was modeled for the two groups of animals, and consistent with the empirical data, the k_A for rh-ActA-treated was twice that of vehicle-treated animals. Kinetic constants for follicle formation, follicle loss and follicle expansion from birth to postnatal day 19 were also derived for vehicle and rh-ActA treatment conditions. Importantly, introduction of exogenous rh-ActA revealed an intrinsic ovarian quorum sensing mechanism that controls the number of follicles available at puberty. We propose that there is an optimal number of oocytes present at puberty, and when the follicle number is exceeded, it occurs at the expense of oocyte quality. The proposed mechanism provides a means by which the ovary eliminates excess follicles containing oocytes of poor quality prior to puberty, thus maintaining fertility in the face of abnormal hormonal stimuli in the prepubertal period.

© 2006 Elsevier Inc. All rights reserved.

Keywords: Primordial follicles; Germ cells; Activin; Follicle counts; Oogonia; Oocyte; SSEA-1

Introduction

Establishment and organization of the initial ovarian follicle pool are critical to normal fertility in adult mammals. The balance between germ cell, oocyte and primordial follicle formation and persistence is essential for preventing excessive germline loss leading to ovarian dysgenesis and premature ovarian failure (Guigon and Magre, 2006). During mouse embryonic development, gonadal structures called germline

* Corresponding author. Northwestern University, Department of Neurobiology and Physiology, O.T. Hogan 4-150, 2205 Tech Drive, Evanston, IL 60208, USA. Fax: +1 847 491 2224.

E-mail address: tkw@northwestern.edu (T.K. Woodruff).

¹ These authors contributed equally to this work.

cysts are created within medullary cords (also termed sex cords or ovigerous cords) surrounded by a basement membrane shortly after primordial germ cells (PGCs) reach the genital ridge (10.5–11.5 dpc) (McLaren, 2000) (Fig. 1). The PGCs, more specifically termed oogonia in the female, cluster in the gonad and multiply extensively for the next few days, with a generation time of 15–16 h (Tam and Snow, 1981). The dividing oogonia are held together by intracellular bridges as a result of incomplete cytokinesis to form clonal clumps of 32 cells that tend to go through mitosis synchronously (Gondos, 1973; Pepling and Spradling, 1998) (Fig. 1). Around 13.5 dpc in the female mouse, the first wave of oogonia enter meiosis and eventually arrest as diplotene oocytes close to birth (Anderson and Hirshfield, 1992; Evans et al., 1982; Peters, 1970). Importantly, the onset of meiosis is not a synchronized event—many oogonia continue to mitotically divide whereas others enter meiotic prophase I (Evans et al., 1982). The intrinsic vs. somatic cell-derived signals that influence the meiotic entry of oogonia are areas of intense investigation.

Twenty-four hours after birth (19.5 dpc) in the mouse and approximately 21 weeks of gestation in the human and macaque, species-specific numbers of primordial follicles are assembled from pre-existing germline cysts (Bayne et al., 2004; Eddy et al., 1981; Francavilla et al., 1990; Konishi et al., 1986; Pepling and Spradling, 1998, 2001; Van Wagenen and Simpson, 1965). The transition of the germline cyst into individual follicles occurs when the cysts undergo programmed breakdown (Fig. 1). A small fraction of selected

oocytes undergo a wave of atresia whereas the surviving oocytes become surrounded by proliferating somatic cells (pregranulosa cells) that invade the cyst, divide the cytoplasm and eventually guide the separation of oocytes to form individual follicles (Hirshfield, 1991; Pepling and Spradling, 2001). Associated with meiotic prophase and continuous with cyst breakdown is a massive loss in germ cell number (Borum, 1961; McClellan et al., 2003; Pepling and Spradling, 2001; Prepin et al., 1985). The factors that control this balance of germ cell loss with the number of postnatal follicles that emerge from the starting pool of germ cells are not known. Moreover, how initial follicle numbers impact adult fertility has not been fully explored in the mouse.

Steroid and peptide hormones, as well as endocrine disruptors, control or interrupt adult follicle maturation and selection and are therefore good candidate modulators of the initial follicle pool. One peptide hormone known to be involved in mouse and human follicle formation *in vitro* is activin. Activin and its receptors are expressed in the genital ridge at the time of germ cell colonization and proliferation (Feijen et al., 1994), and the XX gonad expresses the activin antagonist inhibin B in the 12.5 dpc mouse (Yao et al., 2006). Activin has been shown to organize two-dimensional mouse follicles from monolayer cultures of granulosa cells and oocytes *in vitro*, and these structures are able to synthesize both steroid and peptide hormones (Li et al., 1995). Additionally, activin promotes germ cell proliferation prior

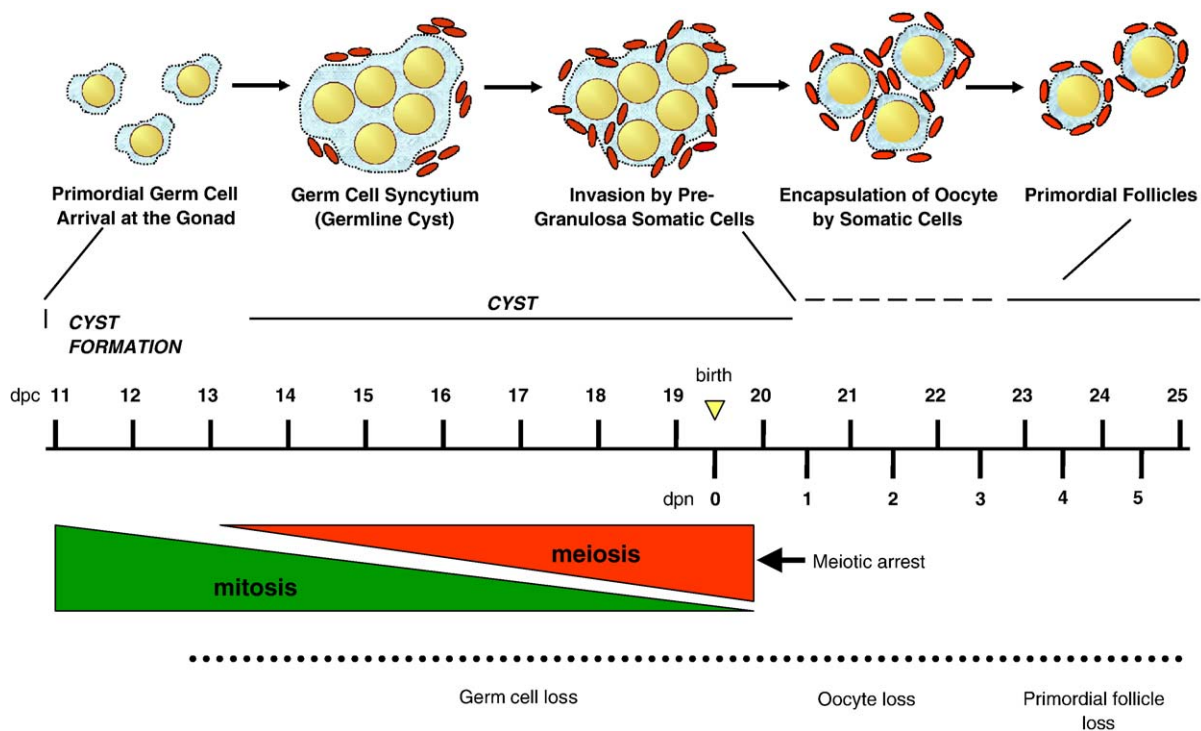


Fig. 1. Schematic of germline cyst formation, breakdown and primordial follicle formation. Following PGC arrival at the gonad, germline cysts form between 10.5 and 13.5 dpc. During cyst formation, mitotic division is accompanied by incomplete cytokinesis so that the daughter cells remain connected by intercellular bridges. Around 13.5 dpc, the first wave of oogonia within the cysts enter meiosis and arrest at the end of prophase I. Approximately 24 h after birth, these cysts begin to breakdown as somatic cells invade and begin to encapsulate individual oocytes into primordial follicles. Coincident with cyst breakdown is an initial loss of germ cells followed by primordial follicle loss. dpc=days postcoitum, dpn=days postnatal.

to the formation of primordial follicles in human fetal ovarian cortical cultures, making it a potential regulator of the earliest events in the ovary (Martins da Silva et al., 2004). Accordingly, loss of activin through gene knockout, receptor elimination or overexpression of dominant-negative cytoplasmic co-regulators results in gonadal dysgenesis or inappropriate follicle function (Bristol-Gould et al., 2005; Brown et al., 2000; Matzuk et al., 1995; McMullen et al., 2001). Lastly, activin is a potent regulator of cell cycle progression and differentiation in a variety of tissues including the breast, ovary and prostate (Burdette et al., 2005; Dowling and Risbridger, 2000; El-Hefnawy and Zeleznik, 2001; Ogawa et al., 2003; Reis et al., 2004). Therefore, we predicted that activin may regulate the number of follicles formed from germline cysts *in vivo* in the mouse during the critical period of germline cyst breakdown and follicle formation.

The population of follicles present in the ovary on postnatal day 6 represents the total number of oocytes that were encapsulated by pre-granulosa cells and is the total population available to the female, at least until puberty. Recent studies suggest that adult germ cells may be derived from stem cells recruited from the bone marrow and this cohort, not the initial follicle pool, drives fertility later in life (Johnson et al., 2005). Interestingly, activin is also known to induce stem cell differentiation in murine bone marrow cultures (Gaddy-Kurten et al., 2002). To determine whether the initial follicle pool can be manipulated hormonally, and to establish the effect of activin on germ cell proliferation, follicle formation and possible stem cell recruitment, neonatal mice were treated with recombinant human Activin A (rh-ActA) during the critical period of germline cyst breakdown and initial follicle assembly. We then explored changes in postnatal follicle number, oocyte health status and the impact on adult fertility.

Lastly, we developed a mathematical model to substantiate results obtained from rh-ActA injection experiments and to describe germ cell/early follicle dynamics. For the first time, our study design permitted us to describe rates of follicle formation, loss, expansion and atresia during neonatal life in an untreated mouse ovary and compare these values to rh-ActA-treated mouse ovaries. Taken together, our empirical data and mathematical modeling suggest that the initial follicle pool can be regulated by activin during the critical period of germline cyst breakdown and primordial follicle assembly; however, significant alterations to the follicle pool caused by exogenous activin are restored by puberty via an intrinsic ovarian quorum sensing mechanism.

Materials and methods

Animals

CD1 mice were maintained in accordance with the policies of the Northwestern University's Animal Care and Use Committee. Mice were housed, injected and bred in a controlled barrier facility within Northwestern University's Center of Comparative Medicine (Evanston, IL). Temperature, humidity and photoperiod (12L, 12D) were kept constant. Mice were fed a phytoestrogen-free diet (Harlan Teklad Global 2019 or Harlan Teklad Breeder diet 2919, Harlan Teklad, Madison, WI).

Tissue processing and follicle counting

Vehicle- and rh-ActA-treated animal ovaries were fixed for 14 h in 4% paraformaldehyde and processed for paraffin embedding. Ovaries were completely serial sectioned and stained for counting. Based on several approaches by others, we developed a rigorous counting method (Canning et al., 2003; Durlinger et al., 1999; Flaws et al., 2001; Johnson et al., 2004; Pepling and Spradling, 2001; Ratts et al., 1995). Two or more individuals counted 5 μ m serial sectioned ovaries collected on postnatal days 0 (19.5 dpc), 6, 10 and 19. The investigators were blinded to treatment condition or group. Follicles were counted in every 5th section throughout the entire ovary (for a discussion of the importance of counting multiple sections, see McClellan et al., 2003). Postnatal day 0 ovaries were stained for germ cell nuclear antigen 1 (GCNA-1, a gift from Dr. George Enders, University of Kansas Medical Center; Enders and May, 1994) in order to visualize and count germ cell nuclei within a cyst. On postnatal days 6, 10 and 19, all follicle types were categorized by morphological criteria. Primordial follicles were classified as an oocyte partially surrounded by either squamous granulosa cells or an oocyte partially surrounded by squamous and cuboidal granulosa cells. Large numbers of morphologically unhealthy primordial follicles were not observed, so all follicles were counted. Primary follicles contained a small oocyte completely surrounded by a single layer of cuboidal granulosa cells. All primordial and primary follicles were counted, regardless of the presence or absence of the oocyte nucleus. Secondary follicles contained a larger oocyte and more than one layer of granulosa cells, with theca cells often present. Tertiary (small antral) follicles were similar in size to secondary follicles but included an antrum. Antral follicles were the largest follicles and contained large antral spaces. Only morphologically healthy secondary, tertiary and antral follicles were counted. Additionally, only sections in which an oocyte nucleus was present were counted to prevent double counting.

The number of follicles per ovary was summed for each observer and that total was averaged. The average number of follicles per ovary was then divided by the number of sections counted in order to calculate follicles per section for each follicle population. Because every 5th section was counted, a correction factor was applied to adjust for the counting rules and the size of the ovary (as ovarian size varied with the age of the animal). To obtain the correction factor for serially sectioned ovaries at each time point, we determined a total standard average section number for each time point. For secondary, tertiary and antral follicles, follicles were only counted if the oocyte nucleus was present in the section. Therefore, these follicles could not be double counted and the follicles per section was multiplied by the average section numbers (see Table 1). On postnatal day 0, germ cell nuclei averaged 7 μ m in size. Therefore, the same nucleus would be detected every 1.5 sections and the average section number was divided by 1.5 (Table 1). For postnatal days 6, 10 and 19, the primordial and primary follicles were counted whether or not the oocyte nucleus was present. The oocyte diameter for these small follicles averaged 14 μ m; therefore, the same follicle would be counted every 2 sections. In order to prevent double counting of these small follicles the average section number was divided by 2 to obtain the normalization factor for these two follicle classes (Table 1). These correction factors were necessary in order to compare follicle pools between time points and to obtain a whole ovary, and then whole animal ($\times 2$), value. Follicle counts were comparable to previous reports using stereological approaches after strain differences were taken into account (Myers et al., 2004). Germ cell counts in CD1 mice on the day of birth were remarkably similar to those obtained in CBA/Ca mice (Faddy et al., 1987).

Activin clearance and targeting

Postnatal day 4 animals were treated with [125 I] rh-ActA to determine ligand clearance and targeting in the ovary. 0.5 h before treatment with iodinated hormone, animals received 50 mg sodium iodide to minimize non-specific uptake of 125 I. 60 μ g/kg of [125 I] rh-ActA was subcutaneously injected into each pup ($n=3$ for each time point). At various times, serum and ovaries were collected. Serum was run on a 12% SDS-PAGE gel, dried and exposed to film in order to obtain hormone clearance information. Five-micrometer serial sections of ovaries were cut using a microtome and slides were dipped in NTB2 emulsion (Eastman Kodak, New Haven, CT) and kept in the dark for 1 month. Following emulsion coating, slides were developed using D-19 Developer (Eastman Kodak, New Haven, CT) and Fixer (Eastman Kodak, New Haven,

Table 1
Normalization factors and follicle counts for vehicle- and rh-ActA-treated CD1 mice

Age (days)	n=ovaries	Normalization		Number of germ cell nuclei or follicles per animal ^a						
		GCN/PF/1°	2°/3°/Antral	GCN	PF	1°	2°	3°	Antral	
0	10	26.7	N/A	16788±1384	N/A	N/A	N/A	N/A	N/A	
<i>Vehicle</i>										
6	11	37.5	75	N/A	10,265±489	414±29	447±49	N/A	N/A	
10	8	50.0	100	N/A	8662±660	567±82	984±85	10±6	N/A	
19	6	62.5	125	N/A	5127±488	294±21	656±74	293±21	20±5	
<i>rh-ActA</i>										
6	12	37.5	75	N/A	13,009±815 ^b	417±30	542±80	N/A	N/A	
10	10	50.0	100	N/A	11,689±771 ^b	440±52	1118±90	6±3	N/A	
19	10	62.5	125	N/A	4794±440	304±31	501±54 ^b	321±43	44±9 ^b	

^aData are given as average±SEM. Abbreviations used: GCN=germ cell nuclei, PF=primordial follicle, 1°=primary follicle, 2°=secondary follicle, 3°=tertiary follicle, N/A=not applicable. ^bSignificantly different than vehicle, $p<0.05$.

CT) then counterstained with hematoxylin. Dark-field images were obtained using a Leica DM5000 microscope and acquired using OpenLab software (Improvision, Lexington, MA).

Hormone measurements

Serum FSH was measured by radioimmunoassay (RIA, Ligand Assay and Analysis Core Laboratory, Center for Research in Reproduction, University of Virginia, Charlottesville, VA). The FSH RIA had a detection range of 3.5–30.7 ng/ml. The average intra-assay and inter-assay coefficients of variation were 4.6% and 14.4%, respectively.

Immunohistochemistry

Mouse ovaries were placed in 4% paraformaldehyde (Sigma, St. Louis, MO) fixative for 8–14 h. The tissue was then dehydrated and paraffin embedded. Five-micrometer sections were cut with a microtome and mounted on Superfrost-Plus slides (Vector Laboratories, Inc., Burlingame, CA). Slides were deparaffinized in xylene and then rehydrated in a series of ethanol. Antigen retrieval (heat in microwave on high for 7 min, low for 2 min) was performed in 10 mM sodium citrate pH 6 followed by cooling in antigen retrieval solution for 20 min. Slides were washed in Tris-buffered saline–Tween (TBS-T) to permeabilize cell membranes, then incubated in 3% hydrogen peroxide in TBS for 15 min. Endogenous avidin and biotin were blocked using the Avidin–Biotin Blocking Kit (Vector Laboratories, Inc., Burlingame, CA) for 15 min each. This was followed by blocking for 1 h in 10% serum (from the host of secondary antibody) in 3% bovine serum albumin–TBS (BSA–TBS) at room temperature. Sections were incubated overnight in primary antibody diluted in the block solution. The following day, the slides were rinsed in TBS-T and incubated in secondary antibody conjugated to biotin (Vector Laboratories, Inc., Burlingame, CA) in 3% BSA–TBS for 30 min to 1 h. Slides were rinsed in TBS-T prior to adding ABC reagent (Vector Laboratories, Inc., Burlingame, CA) for 30 min. Finally, DAB substrate (Vector Laboratories, Inc., Burlingame, CA) was added for 3 min, the reaction stopped for 5 min in ddH₂O and the slides were counterstained with hematoxylin. Immunohistochemical images were acquired on a Nikon E600 microscope using a Spot Insight Mosaic 11.2 color digital camera (Diagnostic Instruments, Sterling Heights, MI) and ADVANCED SPOT IMAGING software (Version 4.6, Universal Imaging, Downingtown, PA).

Antibodies

The antigens detected by immunohistochemistry were the activin β_A - and β_B -subunits; the activin receptors ActRIB, ActRIIA, ActRIIB; Smad3; germ cell nuclear antigen 1 (GCNA1); stage-specific embryonic antigen 1 (SSEA-1); and B cell leukemia/lymphoma 2 (BCL-2). The primary antibodies used were rabbit polyclonal anti- β_A - and β_B -subunit antibodies (a gift from W. Vale and J. Vaughn, The Salk Institute, La Jolla, CA); goat polyclonal antibodies purchased

from R&D Systems (Minneapolis, MN) directed against ActRIB, ActRIIA and ActRIIB; a rabbit polyclonal anti-Smad3 antibody purchased from Zymed Laboratories (South San Francisco, CA); mAb 10D9G11 rat IgM that recognizes GCNA1 (gift from Dr. George Enders, University of Kansas Medical Center, Kansas City, Kansas); a mouse anti-SSEA-1 monoclonal antibody (Chemicon International, Temecula, CA); and a mouse anti-human BCL-2 monoclonal antibody (DakoCytomation, Denmark). Dilutions of the primary antibodies against the β_A - and β_B -subunits, ActRIB, ActRIIA, ActRIIB, Smad3, GCNA1, SSEA-1 and BCL-2 were 1:100, 1:100, 1:10, 1:25, 1:25, 1:100, neat, 1:50 and 1:50, respectively. The secondary antibodies used were biotinylated rabbit anti-goat, biotinylated goat anti-rabbit or biotinylated rabbit anti-rat (Vector Laboratories, Inc., Burlingame, CA). Because SSEA-1 and BCL-2 were monoclonal antibodies, the secondary antibody from the M.O.M.TM Immunodetection Kit (Vector Laboratories, Inc., Burlingame, CA) was used. DAB substrate was applied followed by hematoxylin counterstaining. All negative controls were included by omitting the primary antibody.

Identification of proliferating and apoptotic cells

Proliferating cell nuclear antigen (PCNA) was stained by immunofluorescence using a PCNA staining kit (Zymed Laboratories, South San Francisco, CA). For immunofluorescent detection, the TSATM-Plus Fluorescein System (Perkin Elmer Life Sciences, Boston, MA) was used via deposition of an FITC-labeled tyramide proximal to the HRP enzyme site. TUNEL staining was performed using the DeadEndTM Fluorometric TUNEL System Kit following the manufacturer's protocol (Promega Corporation, Madison, WI). Slides were mounted with Vectashield containing DAPI (Vector Laboratories, Inc., Burlingame, CA). Immunofluorescent images were acquired on a Nikon E600 microscope using a Spot RT monochrome digital camera (Diagnostic Instruments, Sterling Heights, MI) and Metamorph Imaging Software (Version 4.9; Universal Imaging, Downingtown, PA).

Counting of PCNA immunopositive cells

Total oocytes and total granulosa cells were counted in 3 different fields within 1 section of several ovaries (vehicle $n=4$, rh-ActA $n=5$). The number of cells counted in each field was similar. Subsequently, PCNA-positive cells were counted in the same fields and the percentage of positive cells out of the total was calculated.

In vivo ovulation (IVO)

IVO was induced on postnatal day 21 or 54 in rh-ActA- and vehicle-treated animals. Animals were primed with 5 IU of PMSG and then induced to ovulate with 5 IU of hCG 48 h later. Intact cumulus–oocyte complexes were collected from the thin walled portion of the oviduct 14 h after hCG treatment and briefly incubated in 200 μ g/ml hyaluronidase to release the oocytes. Oocytes were classified morphologically based on the presence or absence of a germinal vesicle

and polar body. Oocytes were classified as degenerated if the cytoplasm was fragmented or shrunken from the zona pellucida. Images were captured on an inverted Leica DM IRB microscope (Leica, Bannockburn, IL) equipped with a Photometrics CoolSNAP fx camera (Roper Scientific, Tucson, AZ) and MetaVue 5 image software (Universal Imaging Corporation, Downingtown, PA). Two diameters were measured for each oocyte and averaged to determine oocyte size. Oocytes were then fixed and processed for immunofluorescence as previously described (Hodges et al., 2002). Oocytes were stained with a 1:400 dilution of monoclonal anti- α -tubulin (Sigma, St. Louis, MO), followed by a 1:500 dilution of AlexaFluor 488 goat anti-mouse antibody (Molecular Probes, Eugene, OR) and mounted in VectaShield with DAPI (Vector Laboratories, Inc., Burlingame, CA) to examine the meiotic spindles. Immunofluorescent images were acquired on a Nikon E600 microscope using a Spot RT monochrome digital camera (Diagnostic Instruments, Sterling Heights, MI) and Metamorph Imaging Software (Version 4.9; Universal Imaging, Downingtown, PA). Spindles were classified for congression failure and tubulin morphology by two independent observers who were blinded to the treatment condition and group [$n=32-61$ metaphase I (MI) or metaphase II (MII) oocytes per treatment for postnatal day 24 IVO; $n=8-52$ MI or MII oocytes per treatment for postnatal day 57 IVO].

Statistical analysis

Comparisons for follicle counts, number of oocytes ovulated, oocyte diameter and percentage of PCNA-positive cells were made between rh-ActA and vehicle treatment groups using a two-way t test, with $p < 0.05$ considered statistically significant. The percentage of MII class oocytes, PCNA-positive cells and comparisons for tubulin and chromosome morphologies were analyzed using Fisher's exact test, with $p < 0.05$ considered statistically significant. All statistical calculations were carried out with the software package JMP 4.0.4 (SAS Institute, Cary, NC). Data are represented in figures as average \pm SEM.

Mathematical model of germ cell and follicle dynamics

Germ cell (G) and follicle (F) dynamics are described by Eqs. (1) and (2) below. Transitions between states were modeled with first-order kinetics. The initial pool of germ cells (G^0) either (i) are lost (k_L), (ii) form follicles (k_F) or (iii) proliferate and expand the germ cell pool (k_E). The dynamics of germ cell loss and follicle formation in CD1 mice have been previously characterized (Pepling and Spradling, 2001). Briefly, individual follicles began to appear shortly after birth, and a reduction in the germ cell pool was observed through 22.5 dpc (postnatal day 3). The transition from germ cells to follicles was essentially completed by 25.5 dpc (postnatal day 6). After 25.5 dpc (postnatal day 6), follicles are depleted from the ovary by a process termed atresia (k_A). Equations were solved numerically using an ordinary differential equation solver in Matlab (The Mathworks, Inc., Natick, MA). Total follicle counts were used to fully account for the fate of all germ cells, as counting only primordial follicles would artificially lower the germ cell count by neglecting those germ cells that form primordial follicles and subsequently transition to primary and secondary follicles during this time frame.

$$\frac{dG}{dt} = -k_L G - k_F G + k_E G, \quad (1)$$

$$\frac{dF}{dt} = k_F G - k_A F. \quad (2)$$

Follicle loss following the completion of germ cell depletion and follicle formation was modeled assuming first-order kinetics. Under these constraints, Eq. (2) simplifies to Eq. (3). Total follicle counts for postnatal days 6, 10 and 19 (Table 1) were log transformed and fit to the linearized solution using GraphPad Prism 4.0 (GraphPad Software, San Diego, CA). Values for the follicle loss kinetic parameter (k_A) were significantly greater for rh-ActA-treated animals compared with vehicle-treated animals ($p < 0.05$) based on the statistical methods described in (Zar, 1999).

$$\frac{dF}{dt} = -k_A F. \quad (3)$$

Results

Activin subunit and receptor localization in neonatal mice

Prior to beginning the injection study, the presence of the activin β_A - and β_B -subunits, as well as the activin receptors, was examined in the neonatal mouse ovary. Ovaries from postnatal days 0 to 4 were sectioned and immunostained to determine protein localization. Immunostaining of the activin subunits, β_A (Figs. 2A, B) and β_B (Figs. 2C, D), was robust on all days examined within both somatic cells and oocytes (only days 0 and 4 are shown because similar patterns were detected on all days). Continuous staining observed in the postnatal day 0 ovaries indicated localization within the germline cyst (Figs. 2A and C). By postnatal day 4, the brown stain appeared more discrete, with some protein localizing to the oocyte, but more apparent staining within the granulosa cells surrounding the oocytes (Figs. 2B and D, red boxes). Of note, the first follicles that form as a result of the germline cyst breakdown process appear by postnatal day 4. Thus, the overall localization pattern provides convincing evidence that activin subunits are present in the neonatal ovary during germline cyst breakdown.

The activin receptors (ActRIB, ActRIIA and ActRIIB) were also localized to the oocyte and granulosa cells on postnatal days 0–4. Fig. 3 depicts magnified images of receptor staining on postnatal day 4, which show localization patterns similar to that of the activin subunits (Figs. 3A–C). In addition, the activin receptors were also present in the ovarian surface epithelium (OSE; Figs. 3B, C, arrows). Based on these data, neonatal mouse ovaries are potentially activin-responsive.

Pharmacokinetic analysis, serum FSH measurements and induction of the activin signaling pathway in rh-ActA-treated animals

Female mice were injected with rh-ActA from birth through the completion of germline cyst breakdown. Rh-ActA was delivered for 4 consecutive days by subcutaneous administration every 4 h beginning within the first 3 h of life. A timeline depicting the neonatal injection schedule and subsequent experiments performed throughout this study is provided in Fig. 4. The rh-ActA injection scheme was designed to target the time during which cyst breakdown occurred and primordial follicle formation was initiated. Activin is known to be hepatotoxic when delivered continuously; therefore, this injection strategy was developed based on previous pharmacokinetic studies (Woodruff et al., 1993a,b) to avoid activin accumulation. At 10 min, 30 min and 45 min after injection of iodinated rh-ActA, animals were sacrificed and serum and ovaries were collected (Fig. 5A). Serum was run on a gel and exposed to film to determine the presence of iodinated rh-ActA in the serum. By 45 min, no bands were present on the film; therefore, rh-ActA cleared from the neonatal pup circulation within 30–45 min. To determine if rh-ActA had a direct effect on the ovary, the collected ovaries were sectioned, exposed to emulsion and developed. Rh-ActA targeted the

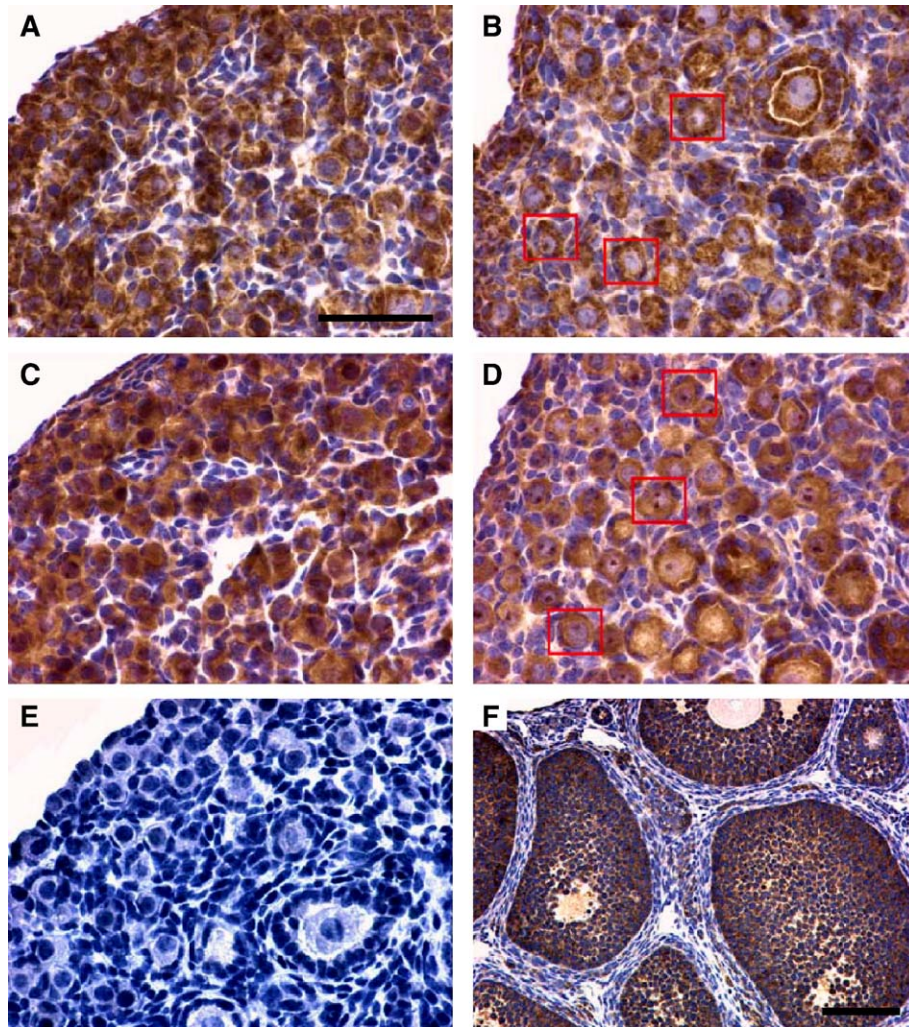


Fig. 2. Actinin subunit localization in neonatal mouse ovaries. β_A -subunit immunostaining on postnatal days 0 and 4 (A, B), respectively, and β_B -subunit immunostaining on postnatal days 0 and 4 (C, D), respectively. Protein is localized in the oocyte and granulosa cells in contact with an oocyte. Staining appears continuous as labeling is evident in oocytes within the germline cysts (A and C). By postnatal day 4, the staining appears more discretely in distinct primordial follicle units; by this time, cyst breakdown has occurred and the initial follicle population is present. Postnatal day 4 negative control in which the β_A -subunit primary antibody was omitted (E). Adult ovary stained for β_A -subunit to indicate specificity of this antibody for granulosa cells (F). Scale bars: 25 μm (A–E) and 100 μm (F).

ovary, specifically the somatic cell compartment, within 10 min of administration (Fig. 5B).

In order to determine if rh-ActA impacted pituitary function, and therefore indirectly acted on the ovary, serum FSH levels were measured in pups injected with rh-ActA or vehicle on postnatal days 2, 6, 10 and 19. No differences in FSH levels were measured in those animals treated with rh-ActA or vehicle, suggesting that exogenous rh-ActA was not acting on the pituitary (Fig. 6A). A characteristic rise in serum FSH was measured on day 10 as described in earlier studies of serum FSH levels in immature female mice and rats (Ackland and Schwartz, 1991; Michael et al., 1980; Rebar et al., 1981). To verify the fact that rh-ActA was bioactive *in vivo*, Smad3 immunoreactivity was measured. Higher levels of nuclear Smad3 were detected in ovaries from rh-ActA-treated animals compared with vehicle-treated animals (Figs. 6B and C). These data indicate that the exogenous ligand not only targeted the ovary but also activated the actinin signaling pathway.

Regulated assembly of the initial follicle pool from germline cysts

To quantitate the baseline number of germ cells present prior to germ cell loss associated with cyst breakdown and follicle formation, GCNA-1 stained nuclei were counted in serially sectioned postnatal day 0 mouse ovaries (Fig. 7). GCNA-1 is a marker of germ cell nuclei, produced until the oocyte arrests in diplotene. A manual counting method (see Materials and methods) was developed to accurately quantify germ cells or follicle populations in an ovary. 16,788 \pm 1384 germ cell nuclei per animal were present in the ovaries of CD1 mice at birth (19.5 dpc, postnatal day 0). By postnatal day 6, few germline cysts were observed and the ovaries contained primarily follicles. At this time, there were 10,265 \pm 489 primordial follicles per animal, 414 \pm 29 primary follicles per animal and 447 \pm 49 secondary follicles per animal (11,126 \pm 504 total follicles). This represents a transition of 66% of the initial germ cell cohort into follicles and a 33% loss of germ cells by postnatal day 6 (Table 1).

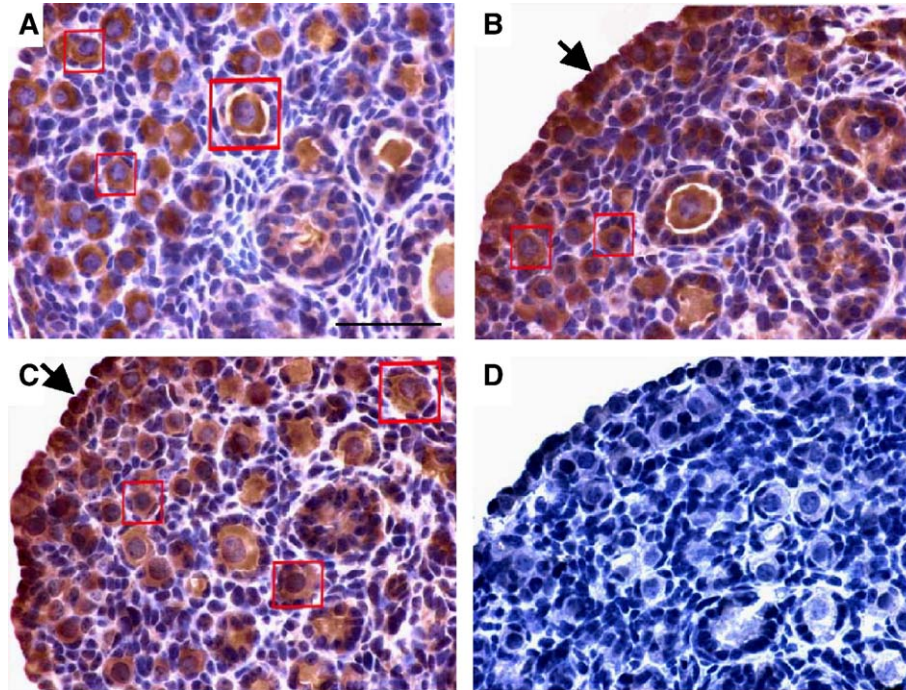


Fig. 3. Actin receptor localization in neonatal mouse ovaries. Actin receptor staining appears localized in a similar manner as that observed for the actin subunits. Postnatal day 4 ovaries immunostained for ActRIB, ActRIIA and ActRIIB, respectively (A–C). The staining is localized in discrete primordial follicles (red boxes). Receptor staining also appears in the OSE of these neonatal ovaries (arrows). Postnatal day 4 negative control in which the ActRIB receptor primary antibody was omitted (D). Scale bar: 25 μ m (A–D).

To examine whether activin regulates follicle assembly, ovaries from rh-ActA injected animals were collected at various intervals following hormone administration and the number and type of follicles were measured (Table 1, Fig. 8). Rh-ActA-

treated ovaries collected on postnatal day 6 had $13,009 \pm 815$ primordial follicles (Figs. 8B and D), a 27% increase in this category compared with vehicle-treated ovaries ($10,265 \pm 489$) (Figs. 8A and C). The primordial follicles were distributed

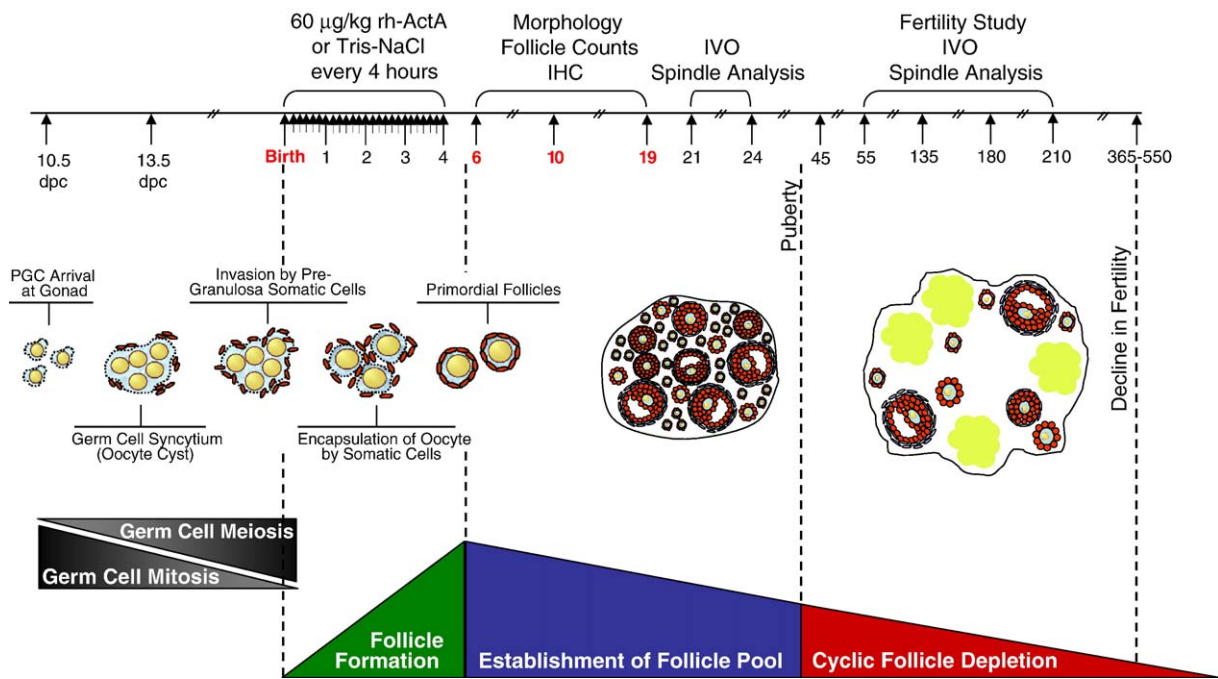


Fig. 4. Neonatal injection study design. Germ cell mitosis and meiosis are processes that take place mainly in the embryonic ovary in the mouse. Prior to birth, germline cysts of interconnected germ cells form by incomplete cytokinesis; shortly after birth, programmed breakdown of these cysts occurs and individual follicles are encapsulated by pre-granulosa cells. At approximately 12 months of age, mice usually show a decrease in fertility due to exhaustion of their ovarian follicular reserve. The red font indicates the days on which germ cell or follicle counts were acquired (birth, postnatal days 6, 10 and 19).

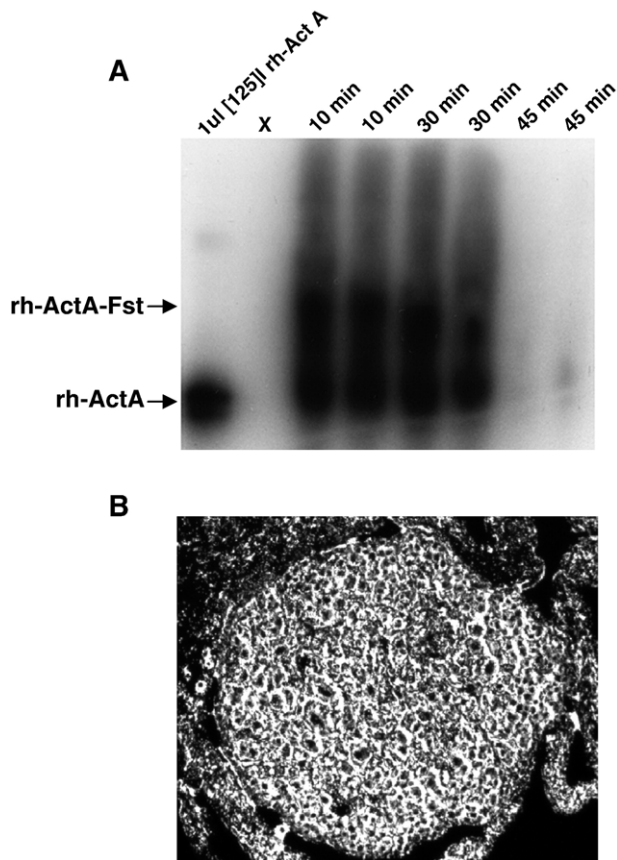


Fig. 5. Pharmacokinetic profile and ligand targeting. (A) At 10 and 30 min after injection, [125 I] rh-ActA is detected in the serum of pups. At 45 min, activin bands are no longer visible. (B) Neonatal ovaries were processed and paraffin embedded to visualize hormone targeting. [125 I] rh-ActA appears to be localized within the somatic cell compartment (shown at 10 min after injection).

throughout the ovary, particularly in the cortical regions of the tissue (Figs. 8C, D). The increase in the initial follicle pool on postnatal day 6 persisted through postnatal day 10, with 35% more primordial follicles present in rh-ActA-treated animal ovaries compared with vehicle-treated animal ovaries (vehicle, 8662 ± 660 vs. rh-ActA, 11689 ± 771 ; Figs. 8E–H). There were no significant differences in the number of primary, secondary or tertiary follicles between treatment groups on postnatal days 6 and 10 (Table 1).

Mechanism of primordial follicle pool expansion

To examine the mechanism by which rh-ActA treatment led to a significant expansion of the primordial follicle pool in postnatal mice, we tested whether rh-ActA treatment was accompanied by a decrease in cell apoptosis, an increase in proliferation or cell survival or whether rh-ActA recruited germline stem cells to the developing ovary at day 2. Similar to previous studies (Fenwick and Hurst, 2002; Pepling and Spradling, 2001), apoptosis (detected by TUNEL staining) was detectable but at very low levels and was not affected by rh-ActA treatment (Figs. 9A–H). The number of FITC-labeled cells was similar between treatment groups. Thus, rh-ActA did not appear to rescue germ cells destined to undergo apoptosis in

the postnatal ovary. Conversely, rh-ActA caused a significant increase in granulosa cell and germ cell proliferation (Figs. 9I–P). We used PCNA, a protein synthesized in early G1 and S phases of the cell cycle, to localize those cells undergoing mitotic activity (counting methods described in Materials and methods). Rh-ActA-treated animals had a 2-fold higher number of PCNA positive somatic cells compared with vehicle-treated animals (42% vs. 23%, $p < 0.001$), suggesting that one mechanism by which rh-ActA regulated follicle number was to increase the number of somatic cells that can encapsulate individual germ cells. Additionally, there was an 8-fold increase in the number of germ cells that were PCNA positive in the ovaries of rh-ActA-treated vs. vehicle-treated animals (40.2% vs. 4.8%, $p < 0.001$). The low level of germ cell mitotic activity measured in postnatal vehicle-treated animals (4.8%) was comparable to the postnatal level of mitosis observed in previous studies in the hamster (Arrau et al., 1981). Moreover, the rh-ActA effect on germ cell proliferation confirms and extends studies performed on *in vitro*-grown human fetal ovarian cortical tissue, in which activin induced germ cell proliferation (Martins da Silva et al., 2004).

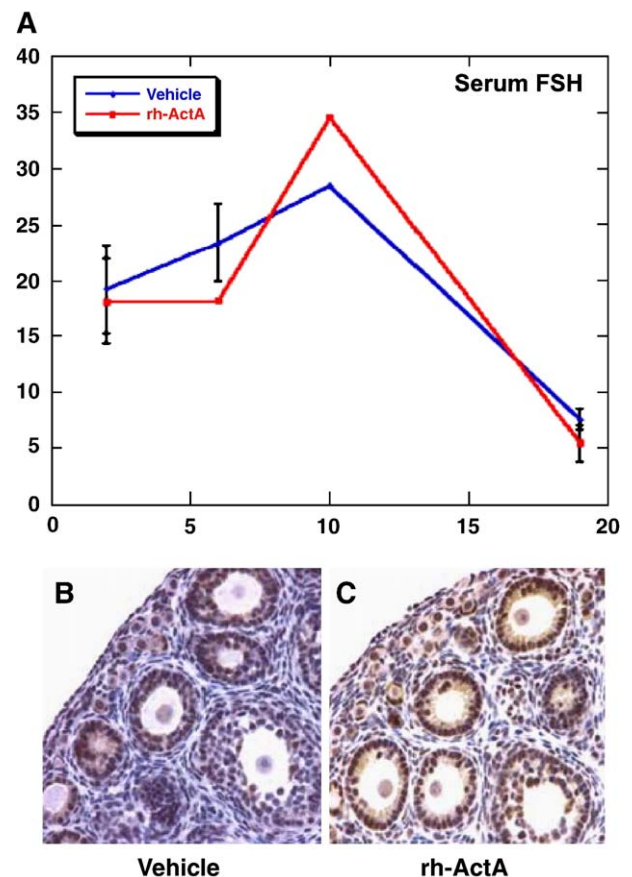


Fig. 6. Serum FSH and Smad3 protein localization. (A) FSH levels in animals of both treatments groups were measured. No significant differences were found using a two-way *t* test ($p < 0.05$). Immunolocalization of Smad3 protein in ovaries of postnatal day 10 vehicle- (B) and rh-ActA-treated (C) animals. A higher intensity of nuclear Smad3 staining was detected in ovaries from the rh-ActA treatment group.

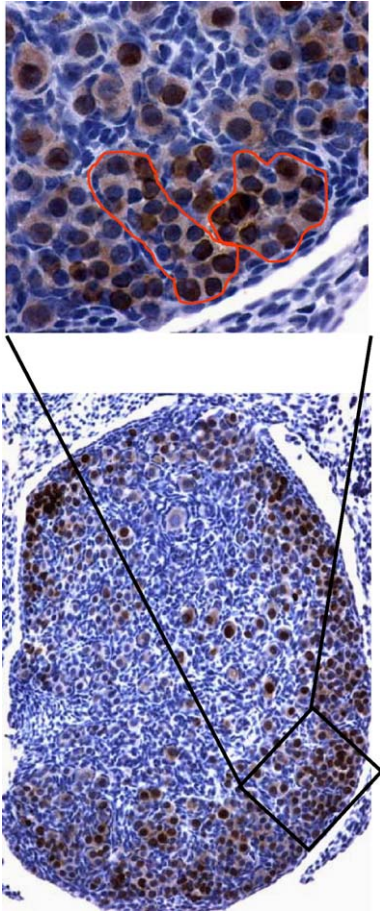


Fig. 7. Germ cell nuclear antigen 1 (GCNA-1) immunostaining. GCNA-1 immunostained ovary at birth (19.5 dpc/postnatal day 0). GCNA serves as a marker of germ cell nuclei until they reach the diplotene stage of the first meiotic division at which time expression is lost. This marker was used to aid in day 0 counting of germ cell nuclei (Table 1).

Recognizing the recently suggested role of peripheral germline stem cells in the repopulation of the primordial follicle pool in the adult ovary (Johnson et al., 2005), we also examined whether rh-ActA induced the recruitment of germline stem cells into the neonatal ovary using the carbohydrate epitope stem cell marker, SSEA-1. No evidence of SSEA-1 staining in vehicle- or rh-ActA-treated ovaries on postnatal day 2 was found (Figs. 10A and B), suggesting that recruitment of stem cells to the neonatal ovary was not responsible for the increase in the initial primordial follicle pool (in the accompanying paper, no germ cell specific SSEA-1 staining was detected in the adult ovary; Bristol-Gould et al. (this issue)).

Finally, the possibility that activin increases follicle survival was examined by anti-apoptotic protein, BCL-2 staining. BCL-2 was found to be highly expressed in the ovary and localized to the oocyte cytoplasm in all follicles, regardless of treatment (Figs. 10C and D). Thus, the mechanism by which activin increases primordial follicle number appears to be stimulation of mitosis in both the somatic cell and germ cell compartments, although we were not able to completely rule out activin inhibition of a mechanism of oocyte loss that does not depend on the BCL-2/BAX pathway.

Effect of rh-ActA on oocyte quality and post-pubertal fertility

By postnatal day 19, the number of primordial follicles in rh-ActA-treated animals was restored to the same levels as that of animals treated with vehicle (Table 1). Rh-ActA-treated ovaries contained significantly fewer secondary follicles, but significantly more antral follicles, compared with vehicle-treated ovaries. Despite the large primordial follicle pool on postnatal days 6 and 10, there were no corresponding increases in the number of later stage follicles, indicating that by postnatal day 19, the ovary appeared to compensate for the excess follicle burden established by rh-ActA administration. These data are similar to previous studies, which illustrated that mouse strain differences in initial follicle number are not maintained in the adult animal (Canning et al., 2003). Additionally, mice that overexpress BCL-2 have an increased number of primordial follicles at birth that are not preserved in later stages of postnatal life (Flaws et al., 2001).

Oocyte quality and adult fertility was further explored to determine whether hormonal modulation of the initial follicle pool impacted these parameters. Immature mice treated with either vehicle or rh-ActA were induced to ovulate on postnatal day 24 with exogenous gonadotropins (*in vivo* ovulation, IVO). Mice treated with rh-ActA had a significantly higher number of oocytes ovulated on postnatal day 24 relative to mice that received vehicle treatment (Fig. 11A, $p < 0.05$). However, ovulated oocytes from animals treated with rh-ActA were less mature, as fewer of these oocytes had advanced to MII (MII %, Fig. 11A, $p < 0.05$) and the oocytes had significantly smaller diameters (7.5% smaller for MI, 10.4% smaller for MII, $p < 0.01$) as compared with oocytes ovulated from vehicle-treated ovaries. Furthermore, when these oocytes were stained for α -tubulin and chromatin, a significantly higher number of the oocytes from rh-ActA-treated mice displayed an excess of tubulin scatter (tubulin spraying away from the spindle body) at the MI stage (Figs. 11B–D). Chromosome alignment was not significantly affected by either treatment (DAPI stain at metaphase plate; Figs. 11C–E). Thus, although rh-ActA-treated mice had a larger number of oocytes that ovulated, oocyte quality (as assessed by oocyte diameter, percentage reaching MII and tubulin scatter) was poor.

To examine the impact of rh-ActA treatment on the initial follicle pool and how it relates to adult fertility, fecundity measurements were taken in mice that were treated in with rh-ActA or vehicle. Based on the oocyte quality findings from the IVO study described above, it was expected that fertility might be affected in the rh-ActA-treated animals. However, rh-ActA-treated animals displayed no significant differences in either the birthing frequency (rh-ActA, 1.2 litters/month vs. vehicle, 1.2 litters/month) or litter size (rh-ActA, 15.9 ± 0.6 pups vs. vehicle, 14.9 ± 1.0 pups) over a 5-month period. These data suggest that by the time of adulthood, and perhaps puberty, poor quality oocytes in the rhActA-treated mice had been eliminated from the ovary.

To test this conclusion directly, treated mice were induced to ovulate at postnatal day 57, which corresponds to the initiation of the breeding study, and gamete quality was tested. There

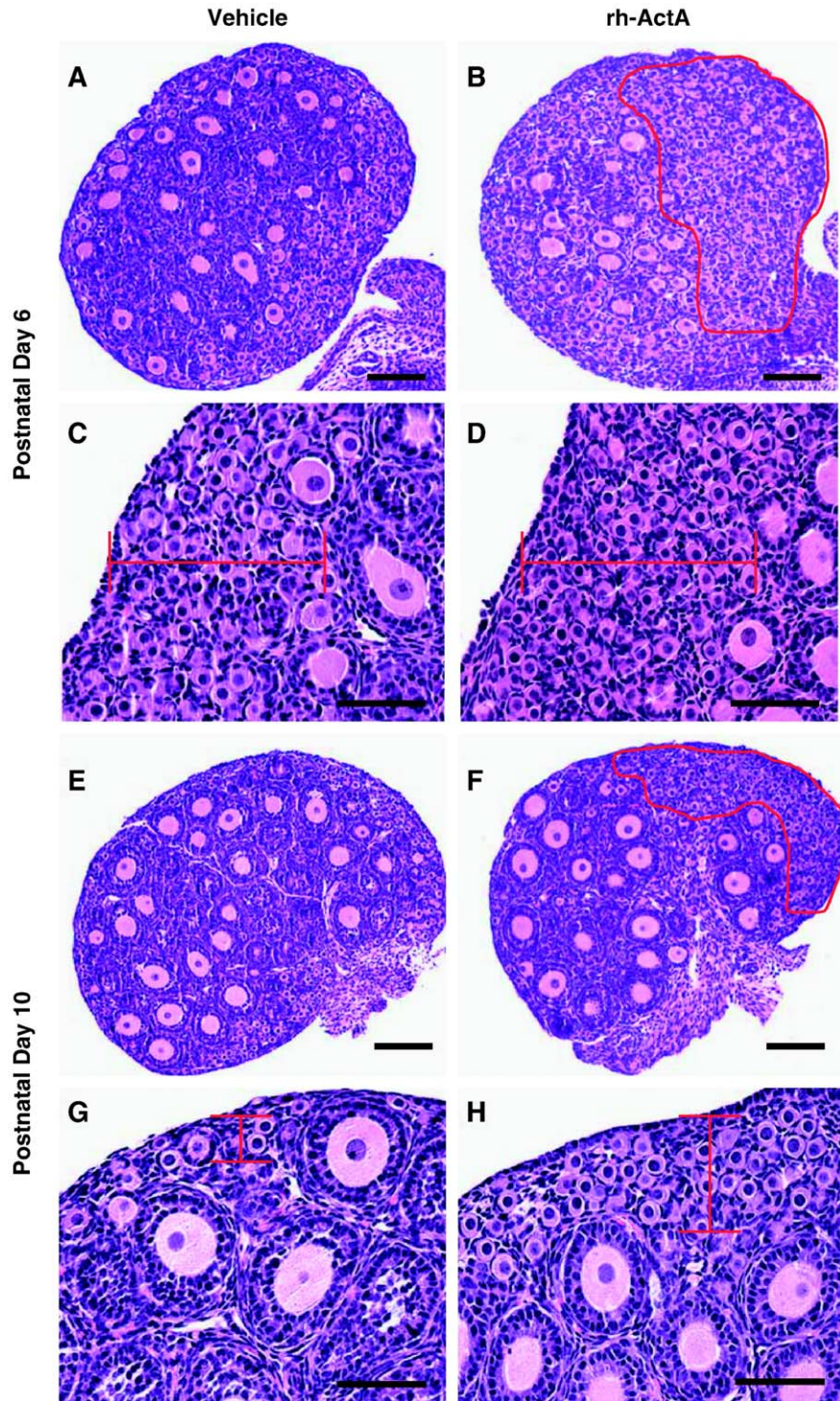


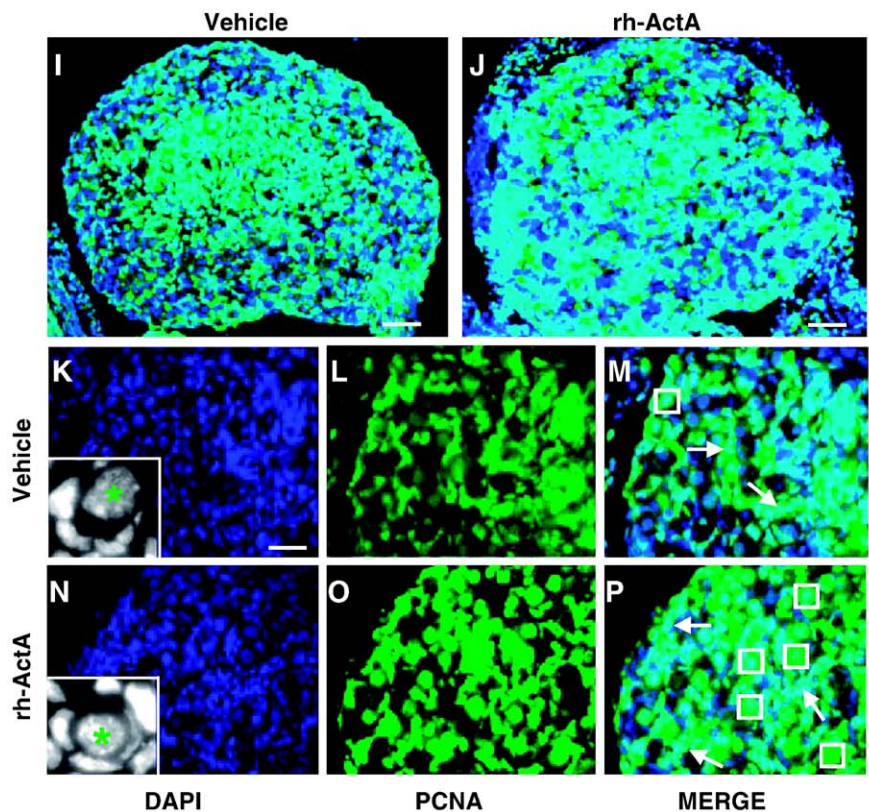
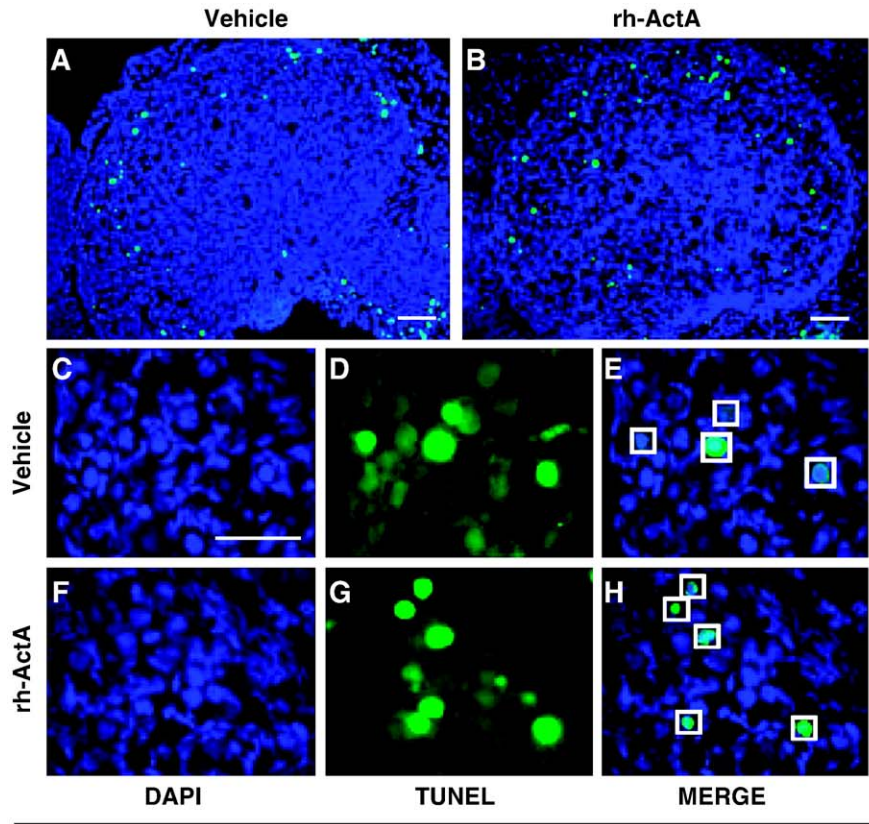
Fig. 8. Ovarian morphology. On postnatal days 6 and 10, there were significantly more primordial follicles (27% and 35% more respectively) in ovaries from rh-ActA-treated mice (A–H). The higher primordial follicle number was observed in cortical regions of ovaries from rh-ActA-treated animals (D, H) compared with those from vehicle-treated animals (C, G) (indicated in red). Scale bars: 100 μm (A, B, E, F) and 50 μm (C, D, G, H).

was no significant difference in the number of oocytes ovulated, the percentage of oocytes that had progressed to MII or the size of oocytes between the two treatment groups (Fig. 11A). Additionally, the percentage of oocytes with tubulin scatter at MI was not significantly different (Figs. 11B and E), indicating that the oocytes ovulated in adult animals

were of similar quality, irrespective of neonatal treatment. These data suggest that the loss of follicles during the highly dynamic prepubertal time frame is an active, not passive, process of sorting the available follicles and eliminating those of poor quality. This ‘sensing’ mechanism would therefore allow every animal to reach puberty with the best possible

cohort of follicles, independent of hormonal or environmental changes that might occur during the critical period of time surrounding germline cyst breakdown and follicle assembly. Additionally, these results are consistent with the idea of an

intrinsic optimal follicle number, an ideal quantity of oocytes that is generated from the finite germline cyst. If this ideal threshold of follicles is exceeded, it appears to be detrimental to gamete quality.



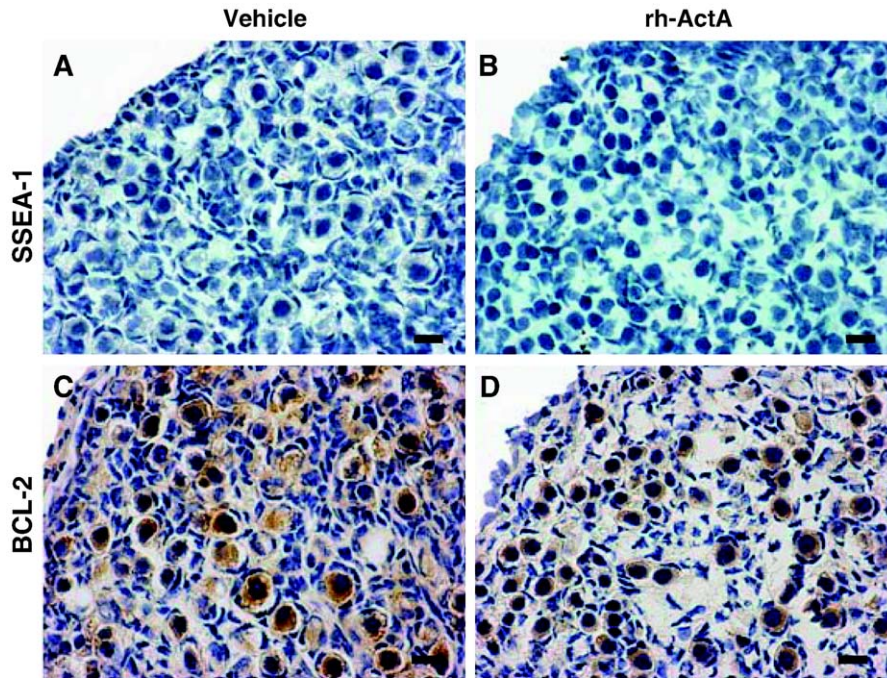


Fig. 10. SSEA-1 and BCL-2 immunohistochemistry on postnatal day 2. Postnatal day 2 ovaries were immunostained to detect stem cell marker SSEA-1 and the cell survival factor BCL-2. No SSEA-1 protein was detected in vehicle-treated (A) or rh-ActA-treated (B) ovaries at this age. BCL-2 protein was detected at similar levels within the oocyte cytoplasm in both treatment groups, (C) vehicle-treated and (D) rh-ActA-treated. Rh-ActA oocytes appeared smaller in panel D, but measurements indicated that oocyte size was similar to that of vehicle-treated animals ($p < 0.05$).

Neonatal germ cell kinetics: kinetics of follicle development under vehicle and rh-ActA treatment conditions

To gain insight into the parameters that control the formation and persistence of the initial follicle pool, a mathematical model was used to simulate germ cell fate through postnatal day 19. We then explored the change in kinetic constants when specific outcomes were altered by addition of hormone. A detailed description of the mathematical modeling can be found in the Materials and methods section.

A set of first-order differential equations was developed to simulate the potential fates of the initial pool of germ cells (Fig. 12). Eq. (1) describes (i) loss by either germ cell lysis/phagocytosis (Franchi and Mandl, 1962) or escape from the ovary (Hiura and Fujita, 1977; Motta and Makabe, 1986; Wordinger et al., 1990) (k_L); (ii) formation of primordial follicles (k_F); or (iii) expansion of the germ cell pool by proliferation of germ cells or recruitment of stem cells (k_E). These germ cell counts were coupled with the follicles formed (k_F) and lost due to atresia (k_A) (Eq. (2)). The equations were solved numerically, applying boundary

conditions for germ cell and follicle number from our counting data through postnatal day 6 and observations from previous studies (Pepling and Spradling, 2001) to determine the various kinetic constants (see Table 2 for complete boundary conditions).

Simulations of germ cell depletion from postnatal days 0 to 6 were performed in two time intervals based on the characteristics of germ cell loss previously described (Pepling and Spradling, 2001). The first interval ranges from postnatal days 0 to 3, during which germ cells are lost or form follicles (represented by the k_L and k_F terms, respectively). An additional term (k_E) was included to account for the possibility of germ cell proliferation and expansion of the germ cell pool. For vehicle-treated animals, PCNA staining indicated approximately 4.8% germ cell proliferation at day 2, which corresponds to a k_E of 0.023 days^{-1} . The second interval ranges from postnatal days 3 to 6, during which germ cell loss is essentially completed (Pepling and Spradling, 2001), and therefore k_L was assumed to be 0. During this time frame, the remaining germ cells form follicles; the rate k_F was assumed to be constant for the entire postnatal days 0–6 time period. During the postnatal days 0–6

Fig. 9. Ovarian apoptosis and cell proliferation in vehicle and rh-ActA-treated animals. (A–H) Levels of apoptosis (detected by TUNEL) were not different between treatment groups. Apoptotic oocytes were FITC labeled whereas cells not undergoing DNA fragmentation were DAPI labeled. (A, C–E) Ovaries from vehicle-treated animals and (B, F–H) ovaries from rh-ActA-treated animals were collected on postnatal day 2 following 48 h of injections. White boxes indicate dual-labeled oocytes. (I–P) Levels of ovarian PCNA staining were higher in rh-ActA-treated animals. (I, K–M) Ovaries from vehicle-treated animals and (J, N–P) ovaries from rh-ActA-treated animals were collected on postnatal day 2 following 48 h of injections. In vehicle-treated animals, little PCNA staining was noted in oocytes, whereas in rh-ActA-treated ovaries, 8-fold more oocytes were PCNA positive (white boxes). There was a 2-fold increase in somatic cell proliferation in ovaries from rh-ActA-treated animals compared with vehicle-treated animals (white arrows). Insets located in panels K and N are monochrome images illustrating how the two cell types (germ cell vs. granulosa cell) were distinguished for counting purposes. The germ cells (green asterisks) are rounder, larger cells compared to the flattened, smaller granulosa cells. Scale bars: 50 μm (A, B, I, J) and 25 μm (C–H, K–P).

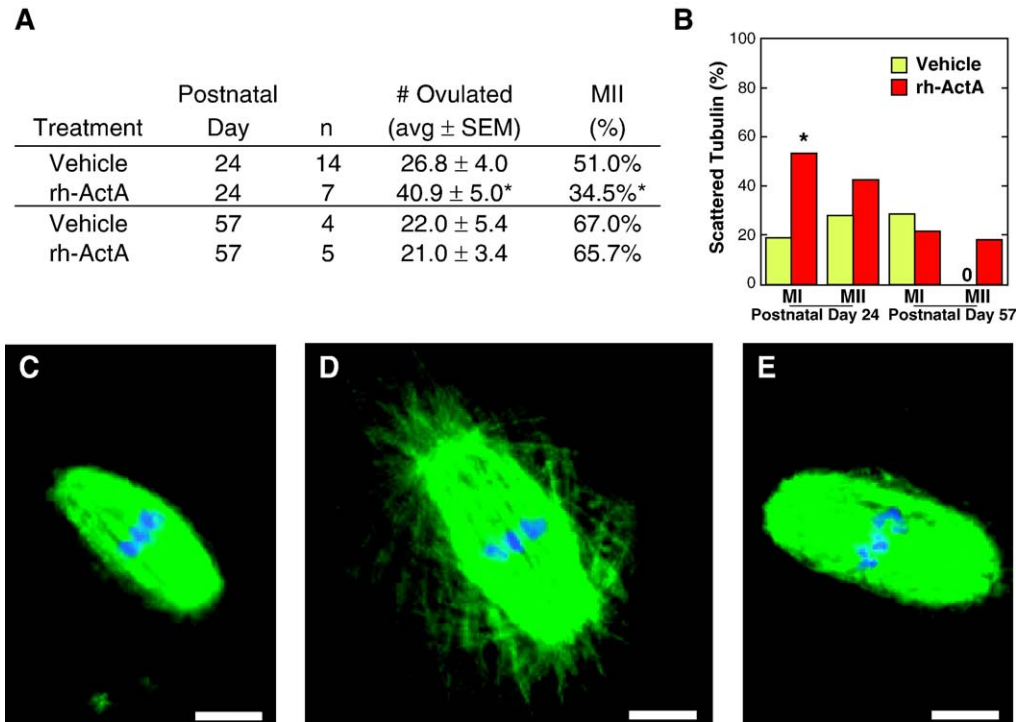


Fig. 11. *In vivo* ovulation and spindle characteristics. (A) On postnatal day 24, rh-ActA-treated animals stimulated to ovulate released significantly more oocytes compared with vehicle-treated animals. However, the oocytes that were ovulated from rh-ActA-treated animals were significantly less mature, as indicated by the percentage that progressed to MII. At postnatal day 57, no differences were observed in the number of oocytes ovulated or the percentage of MII oocytes. *n* = number of animals. (B) Oocytes were immunostained for α -tubulin, an indicator of oocyte health status, and scored based on organization of the meiotic spindle. On postnatal day 24, the rh-ActA-treated animals had significantly more MI and MII oocytes with a scattered tubulin phenotype (*n* = 119 oocytes for rh-ActA, *n* = 68 oocytes for vehicle). The percentage of oocytes with this phenotype was not significantly different between treatment groups at postnatal day 57 (*n* = 36 oocytes for rh-ActA, *n* = 57 oocytes for vehicle). *Significantly different *p* < 0.05. (C–E) Examples of spindle morphology, green (α -tubulin), blue (DAPI). (C) MI oocyte spindle from a vehicle-treated animal on postnatal day 24. (D) MI oocyte spindle from a rh-ActA-treated animal on postnatal day 24. Tubulin is scattered from the barrel shaped spindle. (E) MI oocyte spindle from a rh-ActA-treated animal on postnatal day 57 with organized tubulin. Scale bars: 10 μ m.

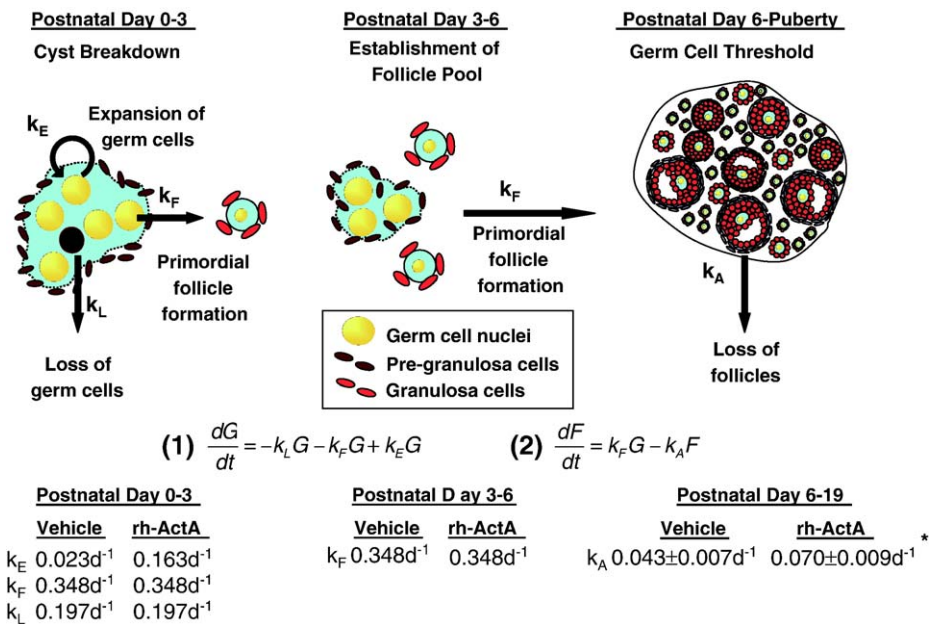


Fig. 12. Mathematical model of germ cell and follicle dynamics. From postnatal days 0 to 3, germ cells undergo three processes; germ cell expansion (k_E), follicle formation (k_F) or loss from the ovary (k_L). Throughout the next 3 days loss subsides and most germ cells complete the transition into primordial follicles, most likely due to pre-granulosa cell invasion. By day 6, after establishment of the initial follicle pool and subsequent growth, larger follicles are depleted from the ovary by a process termed atresia (k_A). *Significantly different, *p* < 0.05.

Table 2
Boundary conditions for mathematical model

Germ cell pool	Follicle pool
$G(\text{day } 0)=G^{\circ}$ (1)	$F(\text{day } 0)=0$
$G(\text{day } 6)=0.1 \times (F^{\circ}/0.9)$ (2)	$F(\text{day } 6)=F^{\circ}$ (3)

(1) Derived from in Table 1.

(2) Based on the previous report that approximately 90% of germ cells at postnatal day 6 have already formed individual follicles (Pepling and Spradling, 2001).

(3) Derived from Tables 1 and 2.

time period, follicle atresia was assumed to be negligible, such that k_A was set to zero.

Simulation of germ cell depletion in rh-ActA-treated animals from postnatal days 0 to 6 were performed using the same time intervals as described for vehicle-treated animals. Using the experimental observation that germ cell apoptosis was similar in the absence or presence of rh-ActA, and assuming that follicle formation rates (although not absolute numbers) would be analogous between vehicle- and rh-ActA-treated animals, it was found that k_E alone was able to account for the differences between the treatment groups. k_E was determined to be 0.163 days^{-1} for the postnatal days 0–3 period, which corresponds to a 38.6% increase in germ cell numbers on postnatal day 2 in the absence of concurrent mechanisms for germ cell loss or follicle formation. This model-derived percentage of germ cell expansion is consistent with the experimentally derived 40.4% PCNA-positive germ cells observed at postnatal day 2. The correlation between the predicted value of k_E and the extent of germ cell mitosis shown by PCNA staining further suggests that the germ cell pool expands through proliferation and not recruitment of germline stem cells to the neonatal ovary.

As the animals approached puberty, differences in the total follicle pool between vehicle- and rh-ActA-treated mice disappeared, with similar numbers of primordial and advanced follicles observed at postnatal day 19. As described above, we hypothesized that the ovary actively eliminates excess follicles in order to meet a pre-determined optimal number by puberty, which is necessary for adult fertility. This depletion of the initial follicle pool was modeled as a first-order process (Fig. 12; Eq. (2)) using total follicle counts from postnatal days 6, 10 and 19. Importantly, the assumption of a first-order process provides that the rate of follicle loss is dependent upon follicle number and is therefore not constant with time. Values for the follicle atresia kinetic parameter (k_A) were significantly greater for rh-ActA-treated animals; the kinetic constant for follicle atresia increased by 62.8% in rh-ActA-treated animals relative to vehicle during the prepubertal period ($p < 0.05$). This validated our prediction that rh-ActA animal ovaries eliminate follicles at a faster rate, possibly to achieve an ideal number of follicles by puberty.

Discussion

The mechanisms governing follicle development in the adult require the interplay of hormones and growth factors that

orchestrate oocyte maturation, somatic cell differentiation and follicular recruitment. In contrast, the factors and mechanisms that manage neonatal follicle assembly and development are less understood. These studies provide new insight into the dynamics of postnatal follicle formation in the prepubertal mouse. First, germline cyst breakdown is a regulated process that can be modulated by exogenous activin. Rh-ActA stimulated both germ cell and granulosa cell proliferation, resulting in an approximate 30% expansion of the primordial follicle pool. Though prepubertal animals treated with rh-ActA ovulated 53% more oocytes, they were of poorer quality than those ovulated by vehicle-treated animals. Despite the initial increase in follicle numbers, there were no differences between treatment groups in the number of ovulated follicles, oocyte quality or litter size in adult animals (2 months old). We propose that an initial follicle pool is established at birth, from which the final follicle pool of puberty is selected. The mechanism(s) governing this previously unrecognized process of prepubertal follicle quality control may be directly regulated by follicle number and oocyte health. When the initial follicle pool number is exceeded and oocyte quality declines, the ovary actively eliminates the excess poor quality oocytes through increased atresia. We propose that this permits the animal to enter puberty with an optimal number of high quality eggs.

The effect of activin on postnatal germ cell mitosis: residual oogonia hypothesis

In addition to stimulating proliferation of the somatic cell compartment, activin also dramatically increased germ cell proliferation on postnatal day 2 based on PCNA detection. It has generally been accepted that the process of germ cell mitosis is completed and followed by meiosis in the embryonic mouse (Bullejos and Koopman, 2004; Evans et al., 1982; Pepling and Spradling, 1998; Zuckerman, 1951). Therefore, by the time of birth, the majority of oocytes are thought to be arrested in diplotene of meiotic prophase (Evans et al., 1982; Tam and Snow, 1981). For the majority of oocytes this is true; however, there is a small percentage of oogonia that have not entered meiosis by the time of birth. We found a baseline proliferation rate of 4.8% in germ cells of vehicle-treated animals (similar to studies in the hamster; Arrau et al., 1981). In other words, approximately 95% of germ cells enter the final stage of meiotic arrest. Intrigued by this observation, we considered the idea that the remaining 5% of proliferating oogonia could be considered stem cells as proposed in previous studies (Johnson et al., 2004, 2005). However, immunostaining with the stem cell marker SSEA-1 provided no evidence that any cells in the neonatal ovary had stem-cell properties. Instead, our data are in agreement with a study in the human fetus, which demonstrated that germ cells that have not yet entered meiosis are mitotically active and that germ cell mitosis continues as other arrested oocytes form primordial follicles (Fulton et al., 2005).

Entry into meiosis occurs in a wave-like fashion in mouse embryonic ovaries. This process is not only dynamic, it is

temporally regulated (Bullejos and Koopman, 2004). Specifically, cells in the rostral portion of the gonad enter meiosis around 13.5 dpc, and meiosis continues to the caudal portion of the ovary over at least the next 48 h. Thus, there is a spatial distribution of the germ cells in the ovary, and we hypothesize that by birth, a small percentage of oogonia have not yet detected or received the signals to enter meiosis whereas other oocytes have already entered meiotic arrest. Because a subset of oogonia is still entering meiosis even at the time of birth, we predict that a cohort of ‘residual’ oogonia may be the target of activin’s proliferative actions.

Clearly additional studies are necessary to determine exact percentages of mitotic oogonia vs. meiotic oocytes within the whole ovary in late gestation and the early neonatal period using additional mitotic markers. PCNA is a marker of DNA replication and widely used for the detection of cell proliferation (Gerdes et al., 1983; Hall and Levison, 1990). However, intensity and thus detection of PCNA expression shows variability according to antibody concentration (McCormick et al., 1993). Therefore, other investigators have used phosphorylated histone H3 to mark mitotic germ cells in the human fetus (Brenner et al., 2003; Fulton et al., 2005). Histone H3 becomes phosphorylated on serine 10 during chromosomal condensation at prophase and is dephosphorylated during telophase (Gurley et al., 1978; Nowak and Corces, 2004). Preliminary immunostaining with this antibody was performed on postnatal day 0 mouse ovaries (Bristol-Gould, unpublished data). A few germ cells per ovarian section were immunopositive for phosphorylated histone H3, but a more quantitative analysis needs to be conducted in addition to co-localization with a germ cell specific marker.

Postnatal loss of oogonia and oocytes via a non-apoptotic mechanism

Of much interest is whether or not oocytes are lost from the ovary via “programmed” cell death or if oocytes die via mechanisms we are unable to detect using conventional methods. High levels of cell loss are measured in the neonatal and prepubertal ovary, but surprisingly, the mechanism of action remains a mystery. The highest frequency of apoptotic cells in the ovary is observed around the time of birth (Baker, 1963; Beaumont and Mandl, 1962; Borum, 1961). Pepling et al. also observed cell apoptosis, particularly in the ovarian outer cortex, prior to the time of cyst breakdown. However, the frequency of labeled germ cells was relatively low compared with the total percent of germ cell loss over the period (Pepling and Spradling, 2001). Almost all germ cell number loss take place during cyst breakdown; consequently, it is puzzling why so few apoptotic germ cells were observed in our study. We predicted that one mechanism by which rh-ActA increased the number of primordial follicles was by decreasing the amount of apoptosis occurring during cyst breakdown and subsequently rescuing germ cells that would otherwise be destined for death. This process was not proven experimentally, however.

A few scenarios may explain the high loss of germ cells without a commensurate correlation to apoptotic markers. First, germ cell death markers may only be expressed for a limited

period of time, such that labeling using traditional methods may not detect a transient cohort that has a short residence time (Pepling and Spradling, 2001). Secondly, it is possible that only a fraction of cells within a cyst undergo programmed cell death, the rest die by an alternate mechanism. Third, it has been proposed that germ cells differentiate and become specialized nurse cells that provide assistance to oocytes destined to be encapsulated—in this scenario, the germ cells “disappear” but do not die (Pepling and Spradling, 2001). Finally, germ cells may die via apoptotic mechanisms but are rapidly cleared from the ovary so that the number of apoptotic cells detected severely underestimates the number of cells that die. These possibilities are worth exploring because germ cell and oocyte loss in the female neonatal mouse is likely a developmentally regulated process distinct from follicular atresia that occurs in the adult animal.

The ‘ovarian quorum sensing’ mechanism

Introduction of exogenous rh-ActA into neonatal animals altered the intrinsic constant for germ cell expansion (k_E). Rh-ActA caused a significant amount of germ cell proliferation and we were able to determine k_E to be 0.163 days^{-1} for the postnatal days 0–3 period, which corresponds to a 38.6% increase in germ cell numbers observed on postnatal day 2. This increase in germ cell number resulted in an increased number of primordial follicles counted on postnatal days 6 and 10 in ovaries from rh-ActA-treated animals; however, by day 19 primordial follicle numbers were similar between rh-ActA- and vehicle-treated groups. We predict that hormonal intervention with activin A altered follicle kinetics by triggering a sense and response mechanism within the ovary that is necessary for maintaining follicle homeostasis and fertility.

We propose that the oocyte sensing ability of the prepubertal ovary is necessary to normalize the follicle cohort by the time of puberty. This mechanism ‘counts’ the number of follicles present. If the follicle number has exceeded a specific threshold or optimal number, atresia is triggered to rid the ovary of the excess follicles. There is evidence of this phenomenon in mice that overexpress BCL-2. These transgenic animals have an increased number of primordial follicles at birth that is not preserved in later stages of postnatal life (Flaws et al., 2001). Using total follicle counts for our treated animals on postnatal days 6, 10 and 19 and solving for the rate of atresia, we determined that the value for the rate of follicular atresia was significantly greater for rh-ActA-treated animals ($p < 0.05$). This suggests that the ovaries of rh-ActA-treated animals eliminated excess follicles to a greater degree than did the ovaries of vehicle-treated animals in order to meet a pre-determined follicle quota by puberty that is necessary for adult fertility. Indeed, this ‘correction’ by the ovary to restore oocyte quality and maintain fertility in the rh-ActA perturbed animals could suggest that either (i) there is an intrinsic compensation within the ovary in response to increased follicle burden which preserves good quality gametes or (ii) the size of the initial follicle pool is of little importance, as might be suggested from the reported existence of germline stem cells (Johnson et al., 2004, 2005).

Our IVO experiment results suggest that there is an ideal quantity of healthy oocytes that can be generated from the finite germline cyst. If this threshold is exceeded, it occurs at the expense of gamete quality/health. Rh-ActA-treated animals had slightly more tertiary, but significantly more antral follicles on postnatal day 19 (Table 1). These follicles appeared to be more responsive to recruitment by administration of gonadotropins. Activin has been shown to stimulate FSH receptor expression, and one possible model for the greater follicle selection seen in rh-ActA-treated mice is that exogenous activin administration may have stimulated FSH receptor content in the developing follicles such that they are more sensitive to the actions of PMSG administered during IVO (Knight and Glister, 2003). Regardless of an increase in FSH responsiveness, though, the oocytes within these follicles were of poorer quality compared with those ovulated by mice treated with vehicle. Oocytes from rh-ActA-treated mice had smaller diameters, were less mature as indicated by the number that progressed to MII and had spindle malformations. We believe that once the follicle quota was exceeded in rh-ActA-treated animals, as indicated by the number of oocytes induced to ovulate, oocyte quality diminished.

Taken together, we conclude that the loss of follicles during the highly dynamic prepubertal time frame is an active, not passive, process necessary for sorting the available follicles and eliminating those in excess. Through this mechanism, oocyte quantity and quality are regulated, such that the suboptimal oocytes present prior to puberty in rh-ActA-treated mice are eliminated, and oocyte quality and fertility are restored by 2 months of age. Such a mechanism for protecting cohorts, within the initial follicle pool, from insult would be critical for adult fertility if this pool is the only source of gametes for fertility. Results in the companion paper (Bristol-Gould et al., this issue) suggest that the initial pool is a sufficient supply of follicles necessary for a lifetime of fertility in the mouse. Therefore, our results indicate that a major drive of the reproductive system is to preserve and extend fertility in order to maximize the opportunity of each animal to place progeny in the future.

Acknowledgments

We kindly thank A. Lisowski and Tyler Wellington within the P01 core facility for sectioning all tissue analyzed in this study. M. Feigon, Q. Freeman and J. Rector contributed to the follicle counting procedures. J. Deck and B. Lai aided in the oocyte spindle analysis. We would like to thank Dr. S. Chapman-Tobin, Dr. C. LaBonne, Dr. J. Burdette and E. West for critically reading versions of the manuscript. Core services of University of Virginia Center for Research in Reproduction Ligand Assay and Analysis Core NICHD (SCCPRR) Grant and U54-HD28934. This work is supported by NIH/NICHD Hormone Signals that Regulate Ovarian Differentiation, P01 HD021921 and the NIH U54 HD41857. S.K.B.-G. was a fellow of the Reproductive Biology Training Grant HD007068. P.K.K. was funded by an NSDEG fellowship.

References

- Ackland, J.F., Schwartz, N.B., 1991. Changes in serum immunoreactive inhibin and follicle-stimulating hormone during gonadal development in male and female rats. *Biol. Reprod.* 45, 295–300.
- Anderson, L.D., Hirshfield, A.N., 1992. An overview of follicular development in the ovary: from embryo to the fertilized ovum in vitro. *Md. Med. J.* 41, 614–620.
- Arrau, J., Roblero, L., Cury, M., 1981. New observations on the onset and duration of the meiotic prophase in the female golden hamster (*Mesocricetus auratus*). *J. Anat.* 132, 627–633.
- Baker, T., 1963. A quantitative and cytological study of germ cells in human ovaries. *Proc. R. Soc. Lond., B Biol. Sci.* 158, 417–433.
- Bayne, R.A., Martins da Silva, S.J., Anderson, R.A., 2004. Increased expression of the FIGLA transcription factor is associated with primordial follicle formation in the human fetal ovary. *Mol. Hum. Reprod.* 10, 373–381.
- Beaumont, H., Mandl, A., 1962. A quantitative and cytological study of oogonia and oocytes in the foetal and neonatal rat. *Proc. R. Soc. Lond., B Biol. Sci.* 155, 557–579.
- Borum, K., 1961. Oogenesis in the mouse. A study of the meiotic prophase. *Exp. Cell Res.* 24, 495–507.
- Brenner, R.M., Slayden, O.D., Rodgers, W.H., Critchley, H.O., Carroll, R., Nie, X.J., Mah, K., 2003. Immunocytochemical assessment of mitotic activity with an antibody to phosphorylated histone H3 in the macaque and human endometrium. *Hum. Reprod.* 18, 1185–1193.
- Bristol-Gould, S.K., Hutten, C.G., Sturgis, C., Kilen, S.M., Mayo, K.E., Woodruff, T.K., 2005. The development of a mouse model of ovarian endosalpingiosis. *Endocrinology* 146, 5228–5236.
- Bristol-Gould, S.K., Kreeger, P.K., Selkirk, C.G., Kilen, S.M., Cook, R.W., Kipp, J.L., Shea, L.D., Mayo, K.E., Woodruff, T.K., 2006. Postnatal regulation of germ cells by activin: the establishment of the initial follicle pool. *Dev. Biol.* (this issue).
- Brown, C.W., Houston-Hawkins, D.E., Woodruff, T.K., Matzuk, M.M., 2000. Insertion of *Inhbb* into the *Inhba* locus rescues the *Inhba*-null phenotype and reveals new activin functions. *Nat. Genet.* 25, 453–457.
- Bullejos, M., Koopman, P., 2004. Germ cells enter meiosis in a rostro-caudal wave during development of the mouse ovary. *Mol. Reprod. Dev.* 68, 422–428.
- Burdette, J.E., Jeruss, J.S., Kurley, S.J., Lee, E.J., Woodruff, T.K., 2005. Activin A mediates growth inhibition and cell cycle arrest through smads in human breast cancer cells. *Cancer Res.* 65, 7968–7975.
- Canning, J., Takai, Y., Tilly, J.L., 2003. Evidence for genetic modifiers of ovarian follicular endowment and development from studies of five inbred mouse strains. *Endocrinology* 144, 9–12.
- Dowling, C.R., Risbridger, G.P., 2000. The role of inhibins and activins in prostate cancer pathogenesis. *Endocr. Relat. Cancer* 7, 243–256.
- Durlinger, A.L., Kramer, P., Karels, B., de Jong, F.H., Uilenbroek, J.T., Grootegoed, J.A., Themmen, A.P., 1999. Control of primordial follicle recruitment by anti-Mullerian hormone in the mouse ovary. *Endocrinology* 140, 5789–5796.
- Eddy, E., Clark, J., Gong, D., Fenderson, B., 1981. Origin and migration of primordial germ cells in mammals. *Gamete Res.* 4, 333–362.
- El-Hefnawy, T., Zeleznik, A.J., 2001. Synergism between FSH and activin in the regulation of proliferating cell nuclear antigen (PCNA) and cyclin D2 expression in rat granulosa cells. *Endocrinology* 142, 4357–4362.
- Enders, G.C., May II, J.J., 1994. Developmentally regulated expression of a mouse germ cell nuclear antigen examined from embryonic day 11 to adult in male and female mice. *Dev. Biol.* 163, 331–340.
- Evans, C.W., Robb, D.I., Tuckett, F., Challoner, S., 1982. Regulation of meiosis in the foetal mouse gonad. *J. Embryol. Exp. Morphol.* 68, 59–67.
- Faddy, M.J., Telfer, E., Gosden, R.G., 1987. The kinetics of pre-antral follicle development in ovaries of CBA/Ca mice during the first 14 weeks of life. *Cell Tissue Kinet.* 20, 551–560.
- Feijen, A., Goumans, M.J., van den Eijnden-van Raaij, A.J., 1994. Expression of activin subunits, activin receptors and follistatin in postimplantation mouse embryos suggests specific developmental functions for different activins. *Development* 120, 3621–3637.

- Fenwick, M.A., Hurst, P.R., 2002. Immunohistochemical localization of active caspase-3 in the mouse ovary: growth and atresia of small follicles. *Reproduction* 124, 659–665.
- Flaws, J.A., Hirshfield, A.N., Hewitt, J.A., Babus, J.K., Furth, P.A., 2001. Effect of bcl-2 on the primordial follicle endowment in the mouse ovary. *Biol. Reprod.* 64, 1153–1159.
- Francavilla, S., Cordeschi, G., Properzi, G., Concordia, N., Cappa, F., Pozzi, V., 1990. Ultrastructure of fetal human gonad before sexual differentiation and during early testicular and ovarian development. *J. Submicrosc. Cytol. Pathol.* 22, 389–400.
- Franchi, L., Mandl, A., 1962. The ultrastructure of oogonia and oocytes in the foetal and neonatal rat. *Proc. R. Soc. Biol.* 157, 99–114.
- Fulton, N., Martins da Silva, S.J., Bayne, R.A., Anderson, R.A., 2005. Germ cell proliferation and apoptosis in the developing human ovary. *J. Clin. Endocrinol. Metab.* 90, 4664–4670.
- Gaddy-Kurten, D., Coker, J.K., Abe, E., Jilka, R.L., Manolagas, S.C., 2002. Inhibin suppresses and activin stimulates osteoblastogenesis and osteoclastogenesis in murine bone marrow cultures. *Endocrinology* 143, 74–83.
- Gerdes, J., Schwab, U., Lemke, H., Stein, H., 1983. Production of a mouse monoclonal antibody reactive with a human nuclear antigen associated with cell proliferation. *Int. J. Cancer* 31, 13–20.
- Gondos, B., 1973. Intracellular bridges and mammalian germ cells differentiation. *Differentiation* 1, 177–182.
- Guigon, C., Magre, S., 2006. Contribution of germ cells to the differentiation and maturation of the ovary: insights from models of germ cell depletion. *Biol. Reprod.* 74, 450–458.
- Gurley, L.R., D'Anna, J.A., Barham, S.S., Deaven, L.L., Tobey, R.A., 1978. Histone phosphorylation and chromatin structure during mitosis in Chinese hamster cells. *Eur. J. Biochem.* 84, 1–15.
- Hall, P.A., Levison, D.A., 1990. Review: assessment of cell proliferation in histological material. *J. Clin. Pathol.* 43, 184–192.
- Hirshfield, A.N., 1991. Development of follicles in the mammalian ovary. *Int. Rev. Cytol.* 124, 43–101.
- Hiura, M., Fujita, H., 1977. Electron microscopic observations on the elimination of the oocyte through the peritoneal epithelium in the neonatal mouse ovary. *Cell Tissue Res.* 182, 73–79.
- Hodges, C.A., Ilagan, A., Jennings, D., Keri, R., Nilson, J., Hunt, P.A., 2002. Experimental evidence that changes in oocyte growth influence meiotic chromosome segregation. *Hum. Reprod.* 17, 1171–1180.
- Johnson, J., Canning, J., Kaneko, T., Pru, J.K., Tilly, J.L., 2004. Germline stem cells and follicular renewal in the postnatal mammalian ovary. *Nature* 428, 145–150.
- Johnson, J., Bagley, J., Skaznik-Wikiel, M., Lee, H.J., Adams, G.B., Niikura, Y., Tschudy, K.S., Tilly, J.C., Cortes, M.L., Forkert, R., Spitzer, T., Iacomini, J., Scadden, D.T., Tilly, J.L., 2005. Oocyte generation in adult mammalian ovaries by putative germ cells in bone marrow and peripheral blood. *Cell* 122, 303–315.
- Knight, P.G., Glistler, C., 2003. Local roles of TGF-beta superfamily members in the control of ovarian follicle development. *Anim. Reprod. Sci.* 78, 165–183.
- Konishi, I., Fujii, S., Okamura, H., Parmley, T., Mori, T., 1986. Development of interstitial cells and ovigerous cords in the human fetal ovary: an ultrastructural study. *J. Anat.* 148, 121–135.
- Li, R., Phillips, D.M., Mather, J.P., 1995. Activin promotes ovarian follicle development in vitro. *Endocrinology* 136, 849–856.
- Martins da Silva, S.J., Bayne, R.A., Cambay, N., Hartley, P.S., McNeilly, A.S., Anderson, R.A., 2004. Expression of activin subunits and receptors in the developing human ovary: activin A promotes germ cell survival and proliferation before primordial follicle formation. *Dev. Biol.* 266, 334–345.
- Matzuk, M.M., Kumar, T.R., Bradley, A., 1995. Different phenotypes for mice deficient in either activins or activin receptor type II. *Nature* 374, 356–360.
- McClellan, K.A., Gosden, R., Taketo, T., 2003. Continuous loss of oocytes throughout meiotic prophase in the normal mouse ovary. *Dev. Biol.* 258, 334–348.
- McCormick, D., Yu, C., Hobbs, C., Hall, P.A., 1993. The relevance of antibody concentration to the immunohistological quantification of cell proliferation-associated antigens. *Histopathology* 22, 543–547.
- McLaren, A., 2000. Germ and somatic cell lineages in the developing gonad. *Mol. Cell. Endocrinol.* 163, 3–9.
- McMullen, M.L., Cho, B.N., Yates, C.J., Mayo, K.E., 2001. Gonadal pathologies in transgenic mice expressing the rat inhibin alpha-subunit. *Endocrinology* 142, 5005–5014.
- Michael, S.D., Kaplan, S.B., Macmillan, B.T., 1980. Peripheral plasma concentrations of LH, FSH, prolactin and GH from birth to puberty in male and female mice. *J. Reprod. Fertil.* 59, 217–222.
- Motta, P.M., Makabe, S., 1986. Elimination of germ cells during differentiation of the human ovary: an electron microscopic study. *Eur. J. Obstet. Gynecol. Reprod. Biol.* 22, 271–286.
- Myers, M., Britt, K.L., Wreford, N.G., Ebling, F.J., Kerr, J.B., 2004. Methods for quantifying follicular numbers within the mouse ovary. *Reproduction* 127, 569–580.
- Nowak, S.J., Corces, V.G., 2004. Phosphorylation of histone H3: a balancing act between chromosome condensation and transcriptional activation. *Trends Genet.* 20, 214–220.
- Ogawa, T., Yogo, K., Ishida, N., Takeya, T., 2003. Synergistic effects of activin and FSH on hyperphosphorylation of Rb and G1/S transition in rat primary granulosa cells. *Mol. Cell. Endocrinol.* 210, 31–38.
- Pepling, M.E., Spradling, A.C., 1998. Female mouse germ cells form synchronously dividing cysts. *Development* 125, 3323–3328.
- Pepling, M.E., Spradling, A.C., 2001. Mouse ovarian germ cell cysts undergo programmed breakdown to form primordial follicles. *Dev. Biol.* 234, 339–351.
- Peters, H., 1970. Migration of gonocytes into the mammalian gonad and their differentiation. *Philos. Trans. R. Soc. Lond., B Biol. Sci.* 259, 91–101.
- Prepin, J., Gibello-Kervran, C., Charpentier, G., Jost, A., 1985. Number of germ cells and meiotic prophase stages in fetal rat ovaries cultured in vitro. *J. Reprod. Fertil.* 73, 579–583.
- Ratts, V.S., Flaws, J.A., Kolp, R., Sorenson, C.M., Tilly, J.L., 1995. Ablation of bcl-2 gene expression decreases the numbers of oocytes and primordial follicles established in the post-natal female mouse gonad. *Endocrinology* 136, 3665–3668.
- Rebar, R.W., Morandini, I.C., Erickson, G.F., Petze, J.E., 1981. The hormonal basis of reproductive defects in athymic mice: diminished gonadotropin concentrations in prepubertal females. *Endocrinology* 108, 120–126.
- Reis, F.M., Luisi, S., Carneiro, M.M., Cobellis, L., Federico, M., Camargos, A.F., Petraglia, F., 2004. Activin, inhibin and the human breast. *Mol. Cell. Endocrinol.* 225, 77–82.
- Tam, P.P., Snow, M.H., 1981. Proliferation and migration of primordial germ cells during compensatory growth in mouse embryos. *J. Embryol. Exp. Morphol.* 64, 133–147.
- Van Wagenen, G., Simpson, M., 1965. *Embryology of the Ovary and Testis: Homo sapiens and Macaca mulatta*. Yale Univ. Press, New Haven, CT.
- Woodruff, T.K., Krummen, L., Chen, S.A., Lyon, R., Hansen, S.E., DeGuzman, G., Covello, R., Mather, J., Cossus, P., 1993a. Pharmacokinetic profile of recombinant human (rh) inhibin A and activin A in the immature rat: II. Tissue distribution of [¹²⁵I]rh-inhibin A and [¹²⁵I]rh-activin A in immature female and male rats. *Endocrinology* 132, 725–734.
- Woodruff, T.K., Krummen, L.A., Chen, S., DeGuzman, G., Lyon, R., Baly, D.L., Allison, D.E., Garg, S., Wong, W.L., Hebert, N., et al., 1993b. Pharmacokinetic profile of recombinant human (rh) inhibin A and activin A in the immature rat. I. Serum profile of rh-inhibin A and rh-activin A in the immature female rat. *Endocrinology* 132, 715–724.
- Wordinger, R., Sutton, J., Brun-Zinkernagel, A.M., 1990. Ultrastructure of oocyte migration through the mouse ovarian surface epithelium during neonatal development. *Anat. Rec.* 227, 187–198.
- Yao, H.H., Aardema, J., Holthusen, K., 2006. Sexually dimorphic regulation of inhibin beta B in establishing gonadal vasculature in mice. *Biol. Reprod.* 74, 978–983.
- Zar, J.H., 1999. *Biostatistical Analysis*. 4th ed. Prentice Hall, Upper Saddle River, NJ (p.360–364).
- Zuckerman, S., 1951. The number of oocytes in the mature ovary. *Recent Prog. Horm. Res.* 6, 63–109.